PCCP

Phenalenyls as tunable excellent molecular conductors and switchable spin filters

Journal:	*Physical Chemistry Chemical Physics*
Manuscript ID	CP-COM-09-2021-004037.R1
Article Type:	Communication
Date Submitted by the Author:	04-Oct-2021
Complete List of Authors:	Smeu, Manuel ; Binghamton University, Physics Monti, Oliver; University of Arizona McGrath, Dominic; University of Arizona

COMMUNICATION

Phenalenyls as tunable excellent molecular conductors and switchable spin filters

Received 00th January 20xx,
Accepted 00th January 20xx

DOI: 10.1039/x0xx00000x

Manuel Smeu,*[a] Oliver L. A. Monti,[b,c] and Dominic McGrath [b]

Phenalenyl-based radicals are stable radicals whose electronic properties can be tuned readily by heteroatom substitution. We employ density functional theory-based non-equilibrium Green's function (NEGF-DFT) calculations to show that this class of molecules exhibits tunable spin- and charge-transport properties in single molecule junctions. Our simulations identify the design principles and interplay between unusually high conductivity and strong spin-filtering.

Creating pure spin current is a fundamental challenge in spintronics, with enormous potential for magnetic storage, low-power electronics, quantum information science, and a fundamental understanding of the interplay between spin and current.[1] Most commonly, spintronic devices such as magnetic tunnel junctions and spin valves make use of carefully engineered stacks of thin magnetic and non-magnetic materials to create, *e.g.,* spin-transfer torque structures.[1] More recently, the use of molecules for creating spin current has received considerable attention: *E.g.*, spin-polarized current may be achieved from transport through chiral molecules.[2,3] Alternatively, all-organic radicals may provide a means for achieving strong spin-filtering and long spin-coherence times at the nanoscale, without the need for external magnetic fields, ferromagnetic electrodes, or transition metal atoms. However, detailed investigation has been hampered by the limited number of stable all-organic radicals.[4–8]

Standard organic spin valve designs require ferromagnetic electrodes and low-temperature operation to achieve significant spin-polarization.[9,10] In such devices, the degree of spin polarization is typically determined by the combination of molecule and electrodes, the "spinterface,"[11] and the spin current originates from the spin-polarized density of states in the electrodes. Alternatively, and without the need for ferromagnetic electrodes, an $S = 1/2$ organic radical may support a spin-split density of states in the junction, leading to tunable differential transmission in the two spin channels.[12]

Here we propose that the single most important aspect of a single-molecule spin filter is the energy level alignment at the molecule-electrode interface, *i.e.*, the extent to which one of the molecular radical orbitals remains singly occupied. We showed previously that charge transfer from the electrodes to the molecule can result in the loss of electron spin polarization in transport, eliminating the spin-filter effect.[13] Here we show how the interplay of charge-transfer, energy level alignment and spin-polarized transport in a new class of stable all-organic radicals enables the design of single molecule junctions with exceptionally high conductance, or high-efficiency and tunable spin filtering.

Efforts to increase electron transmission (conductance) by molecular design have had limited success, attributed in part to Fermi level pinning,[14] an effect that creates a significant injection barrier. The challenge stems from the difficulty in adjusting a frontier molecular orbital (MO) relative to the Fermi energy of the electrodes.[15,16] Many different origins of Fermi level pinning have been discussed, from level broadening due to contact formation, to defects at the interface, and to the existence of interface dipoles.[17–19] One approach to enhance molecular conductance has been in leveraging redox active molecules whose redox state can be controlled by an electrochemical gate to improve conductance, with examples including pyrrolo-tetrathiafulvalene,[20] and DNA.[21] Despite these efforts, overcoming the limitations of Fermi level pinning in molecular electronics remains a barrier to the realization of the true potential of tailored single molecule electronics.

Radicals may offer a solution to this problem. In a spin-restricted picture, the relevant MO is half-filled only, and may be aligned with E_F in thermodynamic equilibrium, conferring metallic character to the molecule,[22] which may offer a route to bypassing the Fermi level pinning problem. Allowing for the two

[a] *Department of Physics, Binghamton University – SUNY. E-mail: msmeu@binghamton.edu*
[b] *Department of Chemistry and Biochemistry, University of Arizona*
[c] *Department of Physics, University of Arizona*

† Electronic Supplementary Information (ESI) available: Computational details of two-probe relaxations and NEGF-DFT calculations; larger set of MOs, spin density, *T*(*E*) peak assignment; charge and spin polarization vs SOMO/SUMO energy; bias-dependent *I-V* and SFE up to 1.0 V. See DOI: 10.1039/x0xx00000x

spins to be different (unrestricted) does not modify this picture substantially, and rather small injection barriers may be realized.[23] This suggests that conductance may be increased by orders of magnitude compared to closed-shell molecules, which has been predicted theoretically for devices based on self-assembled monolayers, and first indications of single molecule devices provide some support for this prediction.[24–26]

In this communication, we investigate a sequence of structurally similar radicals belonging to the class of phenalenyl (PLY) molecules with tailored electronic and spin properties by heteroatom substitution in the ring system, illustrated in Chart 1. For the purposes of this investigation, we restrict ourselves to -SH anchor groups. PLY radicals are known to be stable towards dimerization in solution due to the delocalized spin density;[27,28] synthetic routes are extant for the PLY, 1,3-DAPLY, 4,9-DOPLY and 1,3-DA-4,9-DOPLY cores,[29–32] which proceed from readily available naphthalene derivatives. We employed density functional theory (DFT) to calculate the gas phase MO energies. The molecules were then relaxed between Au electrodes to form two-probe junctions, and we employed the non-equilibrium Green's function technique in conjunction with DFT (NEGF-DFT)[33] to investigate their spin-resolved electron transport properties, including electron transmission spectra, current-voltage characteristics, and spin filter efficiency.

Chart 1. The four phenalenyl class radicals and the closed-shell naphthalene analog.

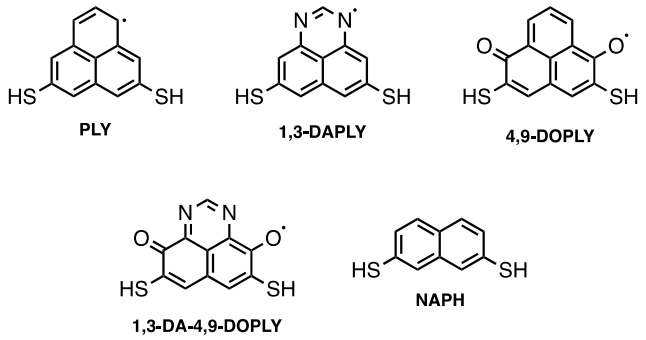

To begin, we calculated the frontier MOs of the four PLY-based radicals in the gas phase. These consist of the singly occupied molecular orbital (SOMO; α spin) and the singly unoccupied molecular orbital (SUMO; β spin), with their corresponding energies in eV, as calculated with the Orca code[34] at the B3LYP/6-311++G(d,p) level of theory[35,36] (Figure 1). We note that there is a substantial SOMO-SUMO gap in the radicals that ranges from 1.5 to nearly 2 eV. While the SOMO and SUMO have the same orbital structure for each radical, the MOs differ greatly across the different radicals, with 4,9-DOPLY and 1,3-DA-4,9-DOPLY supporting substantial amplitude at the anchoring group, while PLY, and 1,3-DAPLY have nodes at the -SH linker group.

The spin-resolved transmission functions [$T(E)$] for these systems were calculated with NEGF-DFT as described in the ESI† (Figure 1). As expected, the α and β transmission spectra are identical for the closed-shell NAPH system. Conversely, all four radicals exhibit spin-polarized transport as can be seen from the spin-split α and β transmission spectra (blue and red plots), particularly near the Fermi energy (E_F). Among the four radicals, all have the SOMO transmission peak just below (to the left of) E_F, and the SUMO peak above E_F, as shown by the blue and red arrows in Figure 1 (the assignment of the transmission peaks is made in Section S2 of the ESI†). While the heteroatom substitution achieves a large difference in SOMO energy of the isolated radicals (left of Figure 1), this only manifests as a small difference in the SOMO transmission peak positions in the junction for the four radicals, aligned just below E_F. In contrast, the SUMO peak positions differ, which results in a varying SOMO-SUMO transmission peak separation across the four radicals. This seemingly subtle point—the position of the SUMO transmission peak relative to the SOMO peak and E_F—is the determining factor that governs the ultimate charge/spin transport characteristics of these radicals, as discussed below.

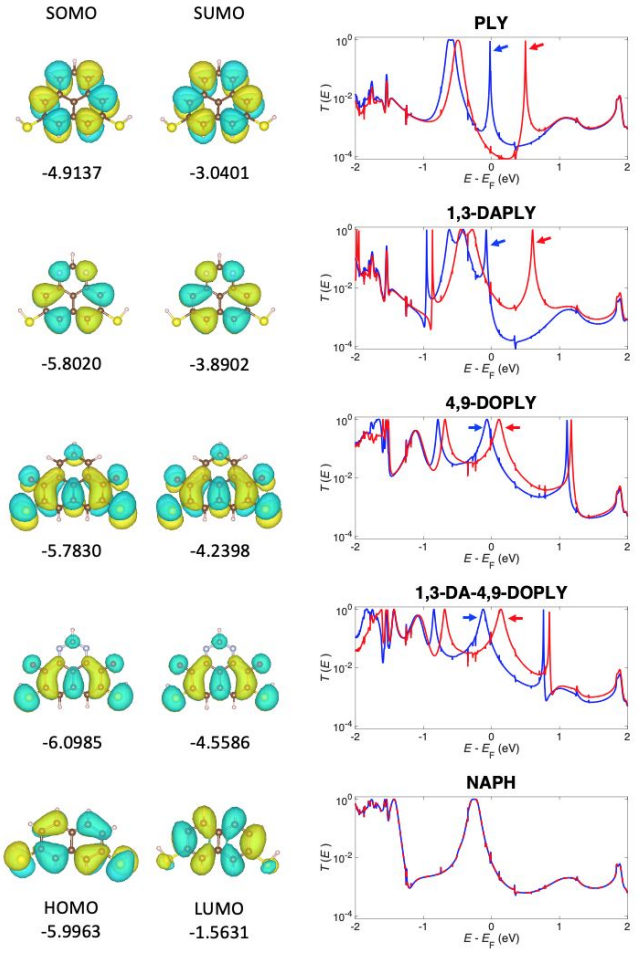

Figure 1. Left: Frontier molecular orbitals for the four radicals (SOMO/SUMO) and the naphthalene molecule (HOMO/LUMO); additional MOs are provided in Figures S2-S6 of the ESI†. The energies (in eV) are listed below each orbital. Right: Spin-resolved transmission coefficient [$T(E)$] for each radical/molecule bridging Au electrodes. Blue/red is for α/β electron transport; the arrows label the SOMO (blue) and SUMO (red) transmission peaks for the radicals.

Also of interest, 4,9-DOPLY and 1,3-DA-4,9-DOPLY have relatively broad SOMO/SUMO peaks, likely resulting from the MO amplitude on the -SH anchoring groups which provide strong coupling to the electrodes, unlike PLY and 1,3-DAPLY which have MO nodes at the anchoring group, resulting in weaker coupling and much narrower transmission peaks (see Figure 1). Therefore, even though some systems (*e.g.*, 1,3-

DAPLY and 4,9-DOPLY) have very similar SOMO energies, they have completely different wavefunctions by simple heteroatom substitution/addition. This manifests both in different electronic coupling to the electrodes (transmission peak width) and ultimately different spintronic behavior. The zero-bias results presented in Figure 1 suggest that all radicals would result in spin-polarized electron transport and high conductance, based on the proximity of the SOMO peak to E_F. To further investigate these systems, we carried out bias-dependent NEGF-DFT calculations (see ESI† for details).

We consider the current as a function of bias voltage (*I-V*) for the four radicals and naphthalene, plotted in Figure 3a. We note that, while all radicals have transmission peaks near E_F (Figure 1), considerably more current flows through 4,9-DOPLY and 1,3-DA-4,9-DOPLY. To understand this result, we turn to the bias-dependent transmission spectra for 4,9-DOPLY (Figure 2a); both the SOMO and SUMO transmission peaks are included in the bias window (grey shaded region) at 0.2 V, which is possible due to the relatively low energy of the SUMO level for this radical. Since the SOMO and SUMO result in broad transmission peaks to begin with (plotted on a linear scale), they yield high transmission and high current through this system. In contrast, the bias-dependent transmission spectra for PLY (Figure 2b) show a larger separation between the SOMO and SUMO peaks, which are also narrower (plotted on a logarithmic scale), resulting in comparatively smaller conductance through this radical.

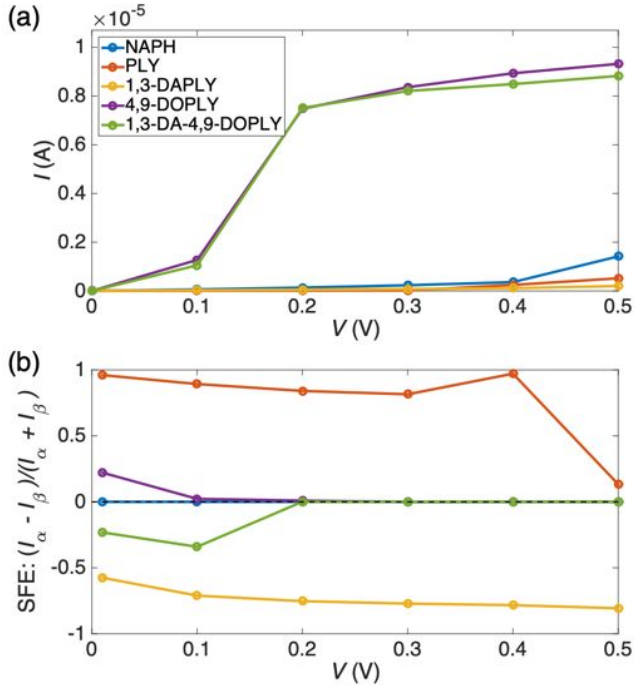

Figure 3. Bias-dependent current (a) and SFE (b) for naphthalene and the four PLY radicals. Two radicals are excellent conductors while the other two make excellent spin filters.

It is apparent that both appropriate energy level alignment and coupling to the electrodes are needed to achieve the partial filling of the two spin-orbitals, resulting in the near-metallic conductance for (1,3-DA-)4,9-DOPLY. At a modest bias of 0.2 V, conductance reaches a value of 0.48 G_0. This is an exceptionally high value for a single molecule coupled to Au electrodes with thiol anchoring groups; even the much smaller system of benzene dithiol exhibits a low-bias conductance of approximately 10^{-2} G_0.[37]

We now turn our attention to spin-transport, and calculate the spin filter efficiency as

$$\mathrm{SFE} = \frac{I_\alpha - I_\beta}{I_\alpha + I_\beta},$$

where α and β represent spin up and spin down channels (assigned arbitrarily). SFE is plotted as a function of bias voltage in Figure 3b. Remarkably, while all four radicals support some degree of spin-polarized current at low bias (0.01 V), only PLY and 1,3-DAPLY maintain a large magnitude of SFE up to 0.4 V; both 4,9-DOPLY and 1,3-DA-4,9-DOPLY entirely lose their SFE by the relatively modest bias of 0.2 V.

The SFE loss behavior of (1,3-DA-)4,9-DOPLY can be understood by inspecting the bias-dependent transmission spectrum. As an illustrative example, Figure 2a shows the transmission spectra as a function of bias for 4,9-DOPLY. The α and β transmission spectra start out different at 0.0 V, but as voltage is increased and the bias window expands (gray shaded region in Figure 2), the SUMO peak (red) is pulled into the bias window, while the bias window is "catching up" to the SOMO peak. At 0.2 V, both the SOMO and SUMO peaks are mostly contained within the bias window, which sets the occupation of each level to a similar value, thereby eliminating the energy splitting between these levels and rendering the α and β energy levels and their resulting transmission spectra spin degenerate. This highlights that a radical that exhibits spin polarized transmission at low bias may not maintain spin polarization even at modest bias. Since many electron transport computational studies are only carried out at zero bias, it is important to stress that this conclusion would be entirely missed without non-equilibrium (finite bias) electron transport calculations.

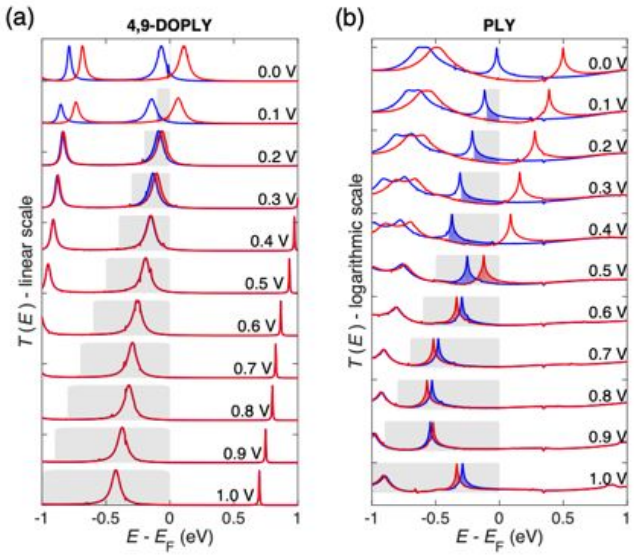

Figure 2. Bias-dependent and spin-resolved transmission spectra for (a) 4,9-DOPLY and (b) PLY radicals. The shaded gray regions enclose the bias window in which the transmission contributes to current. The shaded blue/red regions contain the excess α/β transmission at a given energy within the bias window. Note that (a) uses a linear scale while (b) uses a logarithmic scale for clarity.

As reported previously,[13] the low energy of the SUMO level can lead to the (former) radical accepting an electron from the electrodes, resulting in both SOMO and SUMO becoming occupied, all electrons being paired, and establishing degeneracy of energy levels and their transmission peaks. This is consistent with a charge analysis showing a strong correlation between the charge on the in-junction molecule and the SUMO energy of the isolated molecule (see Figure S7 in the ESI†).

In contrast, the two radicals with the larger SOMO-SUMO transmission peak separation maintain high SFE up to 0.4 V, with values near 0.9 for PLY and -0.8 for 1,3-DAPLY. The bias-dependent transmission spectra for PLY (Figure 2b) illustrate how the α and β transmission spectra remain split, resulting in excess α transmission (shaded blue region) in a given bias window (shaded grey region). However, at 0.5 V the SUMO peak enters the bias window, largely cancelling out the excess α spin transport, thereby reducing SFE. This is the first demonstration of bias-dependent tunable SFE in single molecule electronics. It can be turned on between 0 and 0.4 V, and turned off above 0.4 V, demonstrating tunable spin filtering over an experimentally accessible bias range of ≤ 0.5 V. It should be noted that our calculations did not include a magnetic field. The α spin label is assigned arbitrarily to the majority spin type. In order to initialize the spin state of the radical to a desired value in an experiment, one would need to employ an external magnetic field or ferromagnetic electrodes. Alternatively, optical or spintronic approaches to initialize the radical spin state could also be envisaged.

The extent to which molecular spin filters are possible, and the factors that control the amount of spin polarization, have been rather unclear in the past; some computational investigations suggest that the spin density must be delocalized to achieve spin filtering and spin polarized current,[38] while others point towards the importance of the linker group.[39,40] In most of the PLY family radicals investigated, we find the spin density delocalized over most of the molecule (see Figures S2-S5 in the ESI†), yet $T(E)$ shows the tell-tale sign of strong spin polarization only in PLY and 1,3-DAPLY, suggesting that factors other than spin density are important. In contrast, our work suggests that the key factor that determines spin polarization is the energy level alignment: high spin filter efficiency is achieved if only one of the spin-split radical levels is occupied. Alternatively, nearly complete occupation by an excess electron (or hole), *e.g.*, as with 4,9-DOPLY and 1,3-DA-4,9-DOPLY, collapses the spin-splitting in the transmission function, in exchange for much enhanced molecular conductance.

These classes of single molecule devices can be achieved with judicious heteroatom substitution, allowing for control over the frontier MOs, including SOMO and SUMO, the shape of the MOs, which will affect their coupling to the electrode states, and the ultimate charge and spin transport character of the molecule in-junction. Additionally, different anchoring groups and side groups can be envisaged to further tune electronic properties.

This work suggests that appropriate radicals such as the class of PLY can indeed move beyond Fermi level pinning and exhibit potentially record conductances that have so far only been achieved for special systems with covalent carbon-electrode bonds.[41,42] In the case of those radicals that maintain their radical character when bonded to Au electrodes, these results suggest the possibility of creating tunable spin filters that can be controlled by voltage. This effect may enable the creation of a switchable spin-diode in single molecules without the need of an external magnetic field or ferromagnetic electrodes.

Conflicts of interest

There are no conflicts to declare.

Acknowledgements

This work was performed using the Spiedie High Performance Computing cluster at Binghamton University and the Expanse cluster, a part of the Extreme Science and Engineering Discovery Environment (XSEDE), which is supported by NSF Grant No. ACI-1548562 under allocation TG-DMR180009. We thank Dr. Gökhan Ersan for the TOC graphic. OLAM and DVM acknowledge support from the National Science Foundation (DMR-1708443).

Notes and references

1 A. Fert, *Rev. Mod. Phys.*, 2008, **80**, 1517–1530.
2 B. Göhler, V. Hamelbeck, T. Z. Markus, M. Kettner, G. F. Hanne, Z. Vager, R. Naaman and H. Zacharias, *Science (80-.).*, 2011, **331**, 894–897.
3 R. Naaman, Y. Paltiel and D. H. Waldeck, *J. Phys. Chem. Lett.*, 2020, **11**, 3660–3666.
4 I. Ratera and J. Veciana, *Chem. Soc. Rev.*, 2012, **41**, 303–349.
5 R. Gaudenzi, E. Burzurí, D. Reta, I. D. P. R. Moreira, S. T. Bromley, C. Rovira, J. Veciana and H. S. J. Van Der Zant, *Nano Lett.*, 2016, **16**, 2066–2071.
6 F. Bejarano, I. J. Olavarria-Contreras, A. Droghetti, I. Rungger, A. Rudnev, D. Gutiérrez, M. Mas-Torrent, J. Veciana, H. S. J. Van Der Zant, C. Rovira, E. Burzurí and N. Crivillers, *J. Am. Chem. Soc.*, 2018, **140**, 1691–1696.
7 R. Gaudenzi, J. De Bruijckere, D. Reta, I. D. P. R. Moreira, C. Rovira, J. Veciana, H. S. J. Van Der Zant and E. Burzurí, *ACS Nano*, 2017, **11**, 5879–5883.
8 J. Z. Low, G. Kladnik, L. L. Patera, S. Sokolov, G. Lovat, E. Kumarasamy, J. Repp, L. M. Campos, D. Cvetko, A. Morgante and L. Venkataraman, *Nano Lett.*, 2019, **19**, 2543–2548.
9 T. D. Nguyen, E. Ehrenfreund and Z. V. Vardeny, *Science (80-.).*, 2012, **337**, 204–209.
10 Z. H. Xiong, D. Wu, Z. V. Vardeny and J. Shi, *Nature*, 2004, **427**, 821–824.
11 S. Sanvito, *Nat. Phys.*, 2010, **6**, 562–564.
12 C. Herrmann, G. C. Solomon and M. A. Ratner, *J. Am. Chem.*

Soc., 2010, **132**, 3682–3684.
13 M. Smeu and G. A. Dilabio, *J. Phys. Chem. C*, 2010, **114**, 17874–17879.
14 S. Rodriguez-Gonzalez, Z. Xie, O. Galangau, P. Selvanathan, L. Norel, C. Van Dyck, K. Costuas, C. D. Frisbie, S. Rigaut and J. Cornil, *J. Phys. Chem. Lett.*, 2018, **9**, 2394–2403.
15 B. Kim, S. H. Choi, X. Y. Zhu and C. D. Frisbie, *J. Am. Chem. Soc.*, 2011, **133**, 19864–19877.
16 Z. Xie, I. Bâldea, C. E. Smith, Y. Wu and C. D. Frisbie, *ACS Nano*, 2015, **9**, 8022–8036.
17 M. Oehzelt, N. Koch and G. Heimel, *Nat. Commun.*, 2014, **5**, 4174.
18 D. M. Newns, *Phys. Rev.*, 1969, **178**, 1123–1135.
19 C. Van Dyck and M. A. Ratner, *J. Phys. Chem. C*, 2017, **121**, 3013–3024.
20 R. J. Nichols and S. J. Higgins, *Acc. Chem. Res.*, 2016, **49**, 2640–2648.
21 L. Xiang, J. L. Palma, Y. Li, V. Mujica, M. A. Ratner and N. Tao, *Nat. Commun.*, 2017, **8**, 14471.
22 F. Rissner, Z. Ma, O. T. Hofmann, C. Slugovc, Z. Shuai and E. Zojer, *J. Mater. Chem.*, 2012, **22**, 4269–4272.
23 G. Heimel, E. Zojer, L. Romaner, J. L. Brédas and F. Stellacci, *Nano Lett.*, 2009, **9**, 2559–2564.
24 J. Liu, X. Zhao, Q. Al-Galiby, X. Huang, J. Zheng, R. Li, C. Huang, Y. Yang, J. Shi, D. Z. Manrique, C. J. Lambert, M. R. Bryce and W. Hong, *Angew. Chemie - Int. Ed.*, 2017, **56**, 13061–13065.
25 L. Yuan, C. Franco, N. Crivillers, M. Mas-Torrent, L. Cao, C. S. S. Sangeeth, C. Rovira, J. Veciana and C. A. Nijhuis, *Nat. Commun.*, 2016, **7**, 12066.
26 N. Crivillers, C. Munuera, M. Mas-Torrent, C. Simão, S. T. Bromley, C. Ocal, C. Rovira and J. Veciana, *Adv. Mater.*, 2009, **21**, 1177–1181.
27 P. Li, S. Wang, Z. Wang, C. Zheng, Y. Tang, Q. Yang, R. Chen and W. Huang, *J. Mater. Chem. C*, 2020, **8**, 12224–12230.
28 A. Mukherjee, S. C. Sau and S. K. Mandal, *Acc. Chem. Res.*, 2017, **50**, 1679–1691.
29 K. Goto, T. Kubo, K. Yamamoto, K. Nakasuji, K. Sato, D. Shiomi, T. Takui, M. Kubota, T. Kobayashi, K. Yakusi and J. Ouyang, *J. Am. Chem. Soc.*, 1999, **121**, 1619–1620.
30 Y. Morita, T. Aoki, K. Fukui, S. Nakazawa, K. Tamaki, S. Suzuki, A. Fuyuhiro, K. Yamamoto, K. Sato, D. Shiomi, A. Naito, T. Takui and K. Nakasuji, *Angew. Chemie - Int. Ed.*, 2002, **41**, 1793–1796.
31 Y. Morita, T. Ohba, N. Haneda, S. Maki, J. Kawai, K. Hatanaka, K. Sato, D. Shiomi, T. Takui and K. Nakasuji, *J. Am. Chem. Soc.*, 2000, **122**, 4825–4826.
32 S. Suzuki, Y. Morita, K. Fukui, K. Sato, D. Shiomi, T. Takui and K. Nakasuji, *Polyhedron*, 2005, **24**, 2618–2624.
33 J. Taylor, H. Guo and J. Wang, *Phys. Rev. B*, 2001, **63**, 245407.
34 F. Neese, *Wiley Interdiscip. Rev. Comput. Mol. Sci.*, 2012, **2**, 73–78.
35 D. B. Axel, *J. Chem. Phys.*, 1993, **98**, 5648–5652.
36 C. Lee, W. Yang and R. R. G. Parr, *Phys. Rev. B*, 1988, **37**, 785–789.
37 X. Xiao, B. Xu and N. J. Tao, *Nano Lett.*, 2004, **4**, 267–271.
38 A. Bajaj, P. Kaur, A. Sud, M. Berritta and M. E. Ali, *J. Phys. Chem. C*, 2020, **124**, 24361–24371.
39 G. Rajaraman, A. Caneschi, D. Gatteschi and F. Totti, *J. Mater. Chem.*, 2010, **20**, 10747–10754.
40 M. S. Zöllner, R. Nasri, H. Zhang and C. Herrmann, *J. Phys. Chem. C*, 2021, **125**, 1208–1220.
41 Z.-L. Cheng, R. Skouta, H. Vazquez, J. R. Widawsky, S. Schneebeli, W. Chen, M. S. Hybertsen, R. Breslow and L. Venkataraman, *Nat. Nanotechnol.*, 2011, **6**, 353–7.
42 W. Chen, J. R. Widawsky, H. Vázquez, S. T. Schneebeli, M. S. Hybertsen, R. Breslow and L. Venkataraman, *J. Am. Chem. Soc.*, 2011, **133**, 17160–17163.